Theoretical Study of the Mechanism of Hydrogenation of Side-On Coordinated Dinitrogen Activated by Zr Binuclear Complexes ($[(\eta_5\text{-}C_5Me_4H)_2Zr]_2(\mu_2,\eta^2,\eta^2\text{-}N_2)$)

Hideaki Miyachi, Yasuteru Shigeta, and Kimihiko Hirao*

Department of Applied Chemistry, Graduate School of Engineering, The University of Tokyo, Tokyo, 113-8656 Japan

Received: June 20, 2005; In Final Form: August 10, 2005

The reaction mechanism of the reduction of dinitrogen coordinated side-on to a binuclear Zr complex, $[(\eta_5\text{-}C_5Me_4H)_2Zr]_2(\mu_2,\eta^2,\eta^2\text{-}N_2)$ (T1), was investigated theoretically using a model complex, $[(\eta_5\text{-}C_5H_5)_2Zr]_2(\mu_2,\eta^2,\eta^2\text{-}N_2)$ (A1), employing density functional theory calculations. The effectiveness of A1 in describing T1 was confirmed by comparing the structures, distributions of charge, and frontier molecular orbitals. Our calculations showed that A1 has a twisted structure, resembling that of T1, which results in similar properties. The calculations for A1 and its derivatives on H_2 addition clearly explain the reaction mechanism and the reaction path that T1 follows, as well as the experimentally required reaction conditions. The immediate reaction of the first and second H_2 additions produces $[(\eta_5\text{-}C_5Me_4H)_2ZrH]_2(\mu_2,\eta^2,\eta^2\text{-}N_2H_2)$ (T2), and this is explained by the barrier heights of the reaction, which were calculated to be 20.4 and 10.9 kcal/mol, respectively. The latter barrier was below that of A1 + $2H_2$. Complex T2 may be the initial complex for further H_2 addition under proper conditions, or it could lose one H_2 molecule followed by H migration from the Zr site to the N site. Both reactions are expected to occur, because of the closeness of the barrier heights (25.1 and 36.5 kcal/mol, respectively). Gentle warming is required for further H_2 additions, which can be understood from the energetics as well. The high reactivity of T1 with H_2 has been discussed by the comparison of the calculation of A1 and another complex with different ligands, presenting an interesting indication on the effects of the ligands. These theoretical results and discussion explaining the experiment should provide insight into the nature of the hydrogenation mechanism.

1. Introduction

The activation of the triple bond of molecular nitrogen (N_2) and its chemical transformation into ammonia under mild conditions, such as near room temperature and at low pressure, has presented a challenge to chemists for a century. Nitrogen is inert due to many factors, such as the strength of its triple bond, its large highest occupied molecular orbital (HOMO)−lowest unoccupied molecular orbital (LUMO) gap, and its nonpolarity.[1,2] The well-known Haber−Bosch process accounts for the production of millions of tons of nitrogen compounds annually for industrial and agricultural purposes,[3] and is extremely useful for nitrogen fixation, as heterogeneous catalysis can produce ammonia from atmospheric N_2 and molecular hydrogen (H_2). However, the high temperature and pressure required result in a large energy loss. The biological analogue of this process is the use of nitrogenases, but the reaction rates of biological processes are generally low, and the required conditions, which occur in living organisms, are too strict for industrialization, though they are surely mild. Therefore, many attempts have been made to discover new nitrogen fixation processes under mild conditions that can replace the Haber−Bosch process, but so far there has been no success. A possible solution for a process carried out under mild conditions is the use of homogeneous catalytic reactions.[4] There are examples of homogeneous mononuclear metal complexes with coordinated N_2 that allow for the catalytic protonation of N_2 to ammonia.[5,6] However, direct catalytic reaction of N_2 and H_2 to form ammonia is still challenging.

Recently, the side-on coordination of N_2 to binuclear transition metal complexes has received attention, since it can activate the N−N bond under mild conditions, and can even lead to the cleavage of the bond to form an N−H bond in the presence of H_2. In general, adding H_2 to N_2-coordinated metal complexes results in an exchange of N_2 and H_2, releasing free N_2 and coordinated H_2. In these cases, whether the complexes are mononuclear or binuclear, N_2 is coordinated end-on, which is a more common coordination form than side-on coordination. This can be explained by considering the occupied σ orbitals of the N_2 as σ donors, leading to a weak bond between the N_2 and the metal. In contrast, the activation of the N−N bond of N_2 coordinated side-on to a binuclear metal complex can be explained within the Dewar−Chatt−Duncanson model, with the π donation from the occupied orbitals of N_2 to the metal and a π^* back-donation from the metal to the empty π^* orbitals of the N_2. For this reason, in principle, side-on coordination is only possible for late transition metals, which have doubly occupied π orbitals. Because of this back-donation to the π^* antibonding orbitals of N_2, the N−N bond is both elongated and activated.

The exception to the known general reaction of coordinated N_2 and H_2 was first observed in 1997 by Fryzuk et al.,[7] who used a binuclear Zr complex with a side-on coordinated N_2 and large ringed ligands, $[P_2N_2]Zr(\mu_2,\eta^2,\eta^2\text{-}N_2)Zr[P_2N_2]$ (P1), (where P_2N_2 = $PhP(CH_2SiMe_2NSiMe_2CH_2)_2PPh$ and Ph = phenyl group) and 1−4 atm of H_2. They demonstrated the formation of an N−H bond and a bridging hydride over the course of a period of 7−14 days. Although this complex only reacted with

* Corresponding author. E-mail: hirao@qcl.t.u-tokyo.ac.jp.

10.1021/jp053308r CCC: $30.25
Published on Web 09/09/2005

one H_2 molecule, to the best of our knowledge, this was the first formation of an N−H bond directly from N_2 and H_2.

In 2004, Pool et al. showed that a binuclear Zr complex with a side-on coordinated N_2 and two tetramethylated cyclopentazienyl ligands coordinated to each Zr, $[(\eta_5\text{-}C_5Me_4H)_2Zr]_2(\mu_2,\eta^2,\eta^2\text{-}N_2)$ (T1), was capable of reacting with more than one H_2 molecule in series to form ammonia in a low yield, along with other Zr byproducts.[8] It was observed experimentally that the N−N bond length of the initial complex, T1, was elongated to 1.36 Å from the bond length of free N_2 of 1.09 Å. The complex reacted with the first two H_2 molecules immediately under ambient temperature (22 °C) in 1 atm of H_2 to form $[(\eta_5\text{-}C_5Me_4H)_2ZrH]_2(\mu_2,\eta^2,\eta^2\text{-}N_2H_2)$ (T2). Each N atom of this complex has one N−H bond, and the N−N bond length was elongated to 1.47 Å. The two reactions that T2 undergoes are both interesting. Boiling a solution of T2 in heptane (∼100 °C) for 5 min results in the loss of one equivalent of H_2 and an N−N cleavage producing T3, which has a planar $Zr(\mu_2,\eta^2,\eta^2\text{-}NH)Zr$ structure. With the help of protons from hydrochloric acid, T3 produces two equivalents of NH_4Cl and Zr byproducts, completing the N_2 fixation process.

The more intriguing reaction is the reaction with three more H_2 molecules to produce ammonia and Zr byproducts in 1 atm of H_2 with gentle warming. Therefore, this is the first observed nitrogen fixation process under mild conditions (∼85 °C, 1 atm) using only H_2 and a well-defined Zr complex. Although this process does not use a catalyst, the fact that the reduction of N_2 to ammonia occurred via a direct reaction with H_2 is very important.[9]

This field of research is also attractive to theoretical chemists, and many computational studies have been carried out. Studies on the electronic and structural properties of bare MN_2M complexes (where M = metal atom) indicate that the ground state of ZrN_2Zr is a low spin state.[10] Another important computational study on P1 using a model complex $[p_2n_2]_2Zr(\mu_2,\eta^2,\eta^2\text{-}N_2)$ (A1′) (where $p_2n_2 = (PH_3)_2(NH_2)_2$) was presented by Basch et al., having p_2n_2 instead of P_2N_2 as the ligand coordinated to the Zr.[11−13] Although the Zr−P bond length of Basch et al. was fixed, since the coordinated P and N atoms were not connected in this model ligand, the structurally rigid aspects of the experimental ligand in this model complex were lost. In their ensuing papers, Basch et al. anticipated that complexes with a side-on coordinated N_2 group may be able to react with more than one H_2 molecule before this was confirmed experimentally.[11−13] These are two examples taken from many computational studies,[14−16] and we consider them very useful for continuing work.

In this work, we focused on answering the following questions, "What is the reaction mechanisms of the H_2 additions, as well as the reaction path in Pool et al.'s experiments?" and "Why are experimental conditions such as heating required?" To obtain theoretical answers to these questions, density functional theory (DFT) calculations (discussed in the following section) were carried out using the model complex for the experimentally reported complex, T1. We note that we have followed the mechanism initially predicted by Basch et al.[13] for the first half of the reactions and compared the two model complexes in the discussion. We first confirm the use of the model complex adopted in this paper to ensure the effectiveness of the results. Pool et al. have demonstrated the importance of the initial structure of T1 for H_2 addition in connection with frontier molecular orbitals.[17] Therefore, we compared the calculated results of the initial model complex and T1. In the Results section, we present the calculated data, such as the optimized structures and their energetics. Then, in the Discussion section, we discuss the topics mentioned above, based on the computational results to formulate the reaction mechanism.

2. Computational Procedure

A model complex was used in our calculations, since the structure of T1 is too large to compute all the reactions with the computer resources presently available. Instead of using the experimentally reported T1 complex, we used the model complex $(Cp_2Zr)_2(\mu_2,\eta^2,\eta^2\text{-}N_2H_2)$ (A1) (where $Cp = \eta^5\text{-}C_5H_5$) as our initial complex. The ancillary ligand, Me (CH_3), of $\eta_5\text{-}C_5Me_4H$ was changed to an H atom, meaning that Cp was the ligand coordinated to the Zr. To confirm the effect of these substitutions, we also performed calculations on the experimental T1, T2, T3, and T4 complexes, which were the same as the experimentally isolated complexes.

All the results presented in this paper were calculated using the hybrid DFT functional B3LYP[18−21] implemented in the Gaussian 03 program package,[22] with Los Alamos ECP and LanL2DZ basis set[23−25] for Zr, and the 6-31G* split valence basis sets for the H, C, N, and P atoms. We performed geometry optimizations for the initial reactant, intermediates, transition states (TSs), and the products of the reaction with H_2. When there are no descriptions, the calculated transition states were confirmed to be in the reaction path using a combination of second derivative calculations, intrinsic reaction coordinate (IRC) calculations,[26,27] and geometry optimization.

We assumed that the electronic states of all structures were ground-state closed-shell singlet states, as suggested by previous research, as discussed.[10] We verified this decision by calculating both the singlet and the triplet electronic states of T1 without performing any modeling. The calculated N−N bond length, which is essential for studies of nitrogen reduction, was 1.36 Å for the singlet state and 1.25 Å for the triplet state, compared to 1.38 Å from X-ray crystal structure data. Observing other structural features, we believe that this decision was justified. In addition, the agreement between the geometric structures of the calculated initial complex and the experimental data was very close, showing the sufficiency of the calculation using the DFT functional and basis sets employed.

3. Results

In this section, we will begin by discussing the structure of the initial complex and focus on the changes in structure and energy during each step. All calculated equilibria and transition structures of complexes A, T1, T2, and T3 are shown in Figure 1. The reaction potential energy diagram is shown in Figure 2. The Mulliken atomic charges and the frontier molecular orbitals that are referred to are shown in Table 1 and Figure 3, respectively. From here, the term "A" denotes a series of model complexes based on complex A, with the numeric (e.g., A1) denoting the individual structure in the reaction pathway. Since we are interested in the reduction mechanism of nitrogen, other relevant reactions associated with the complete nitrogen fixation process are discussed in the following section.

3.1. Structures of the Initial Model Complex, Complex A1, and the Experimental Complex, T1. In general, the reactant complex A1 can take various isomeric forms. Pool et al. presented the importance of dihedral angle $X-Zr^1-Zr^2-X$ (where X is the weighted center of the five C atoms of Cp), in connection with the shape of frontier orbitals in their previous work.[17] They have shown that A1 with 0° for $X-Zr^1-Zr^2-X$ (i.e., a nontwisted A1) does not have the same property as T1, which has a twisted dihedral angle. Therefore, to ensure the

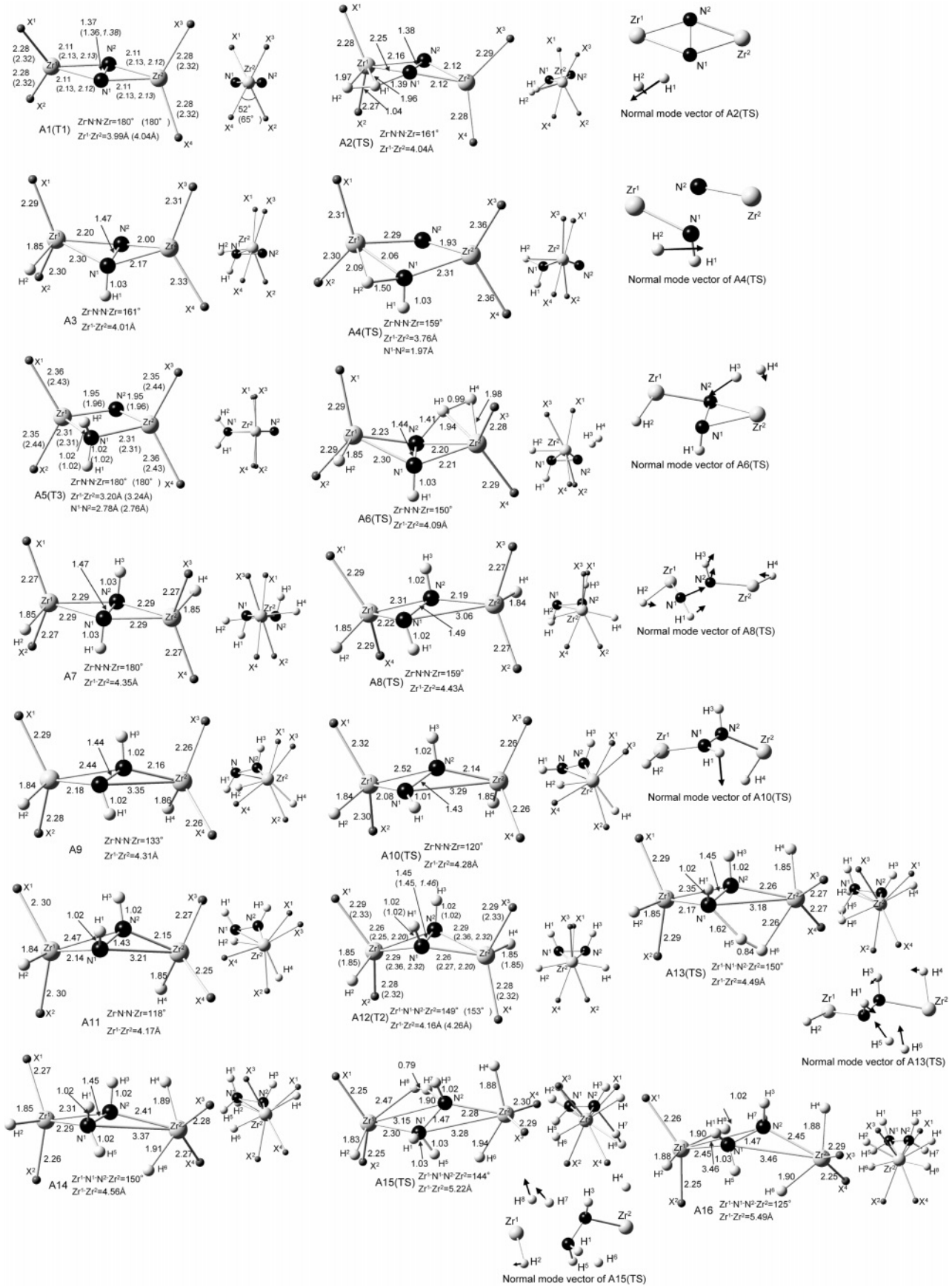

Figure 1. Calculated geometries (in Å) of the initial reactant, transition states, and products of the reaction of complex A1, and experimentally isolated complexes. The numbers in parentheses denote the corresponding values calculated for experimentally isolated complexes. The numbers in italics are the experimentally observed values of isolated complexes. Instead of showing all the atoms of the ancillary cyclopentazienyl ligands, the weighted center, X, of the five C atoms is shown for clarity. Normal-mode vectors of the negative frequencies of transition-state structures are shown as well.

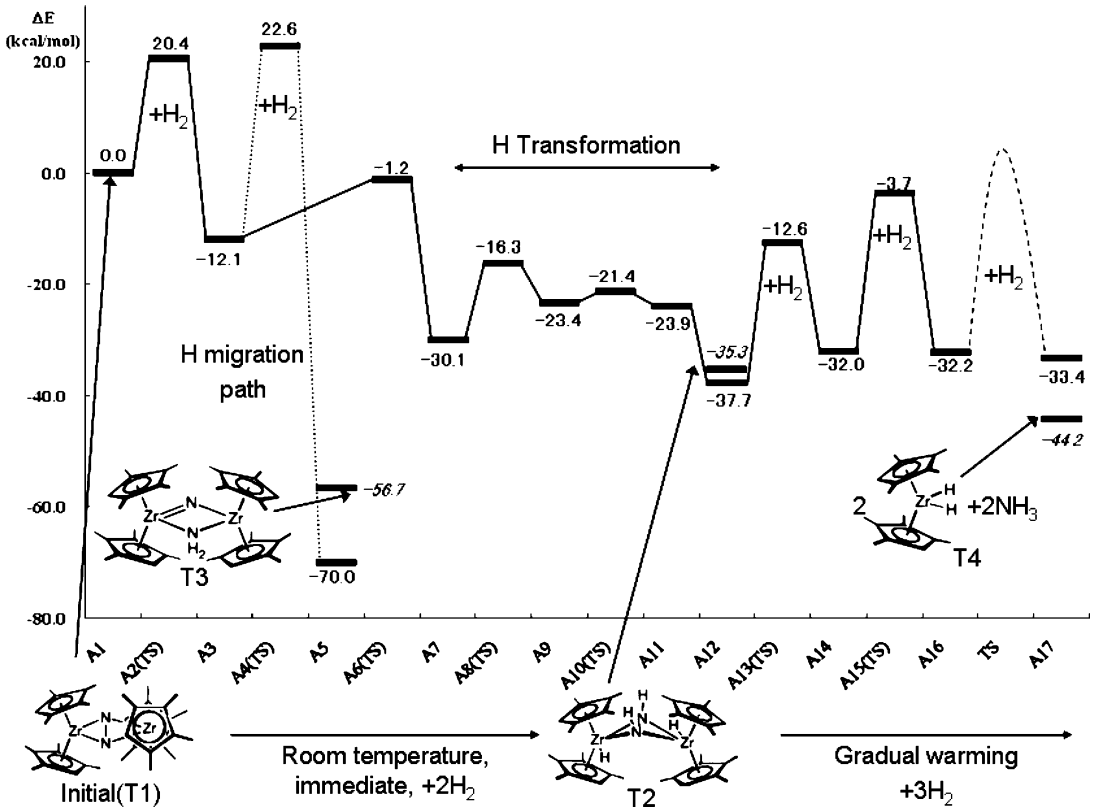

Figure 2. Calculated reaction potential energy diagram of the reactions starting from complex A1. The numbers in italics are the energies from calculations on the experimentally isolated complexes shown in the diagram. The energy for complex A17 is the sum of two equivalents of ammonia and two mononuclear Zr byproducts. An explanation of the experimental conditions is provided in the diagram.

TABLE 1: Calculated Mulliken Atomic Charges of Selected Atoms or Atom Groups of Complexes A1 and T1

	A1	T1
N_1	−0.54	−0.58
N_2	−0.54	−0.57
Zr_1	0.78	0.73
Zr_2	0.78	0.73
Cp[a]	−0.12	−0.08

[a] The presented values of Cp are the sum of (η_5-C_5H_5) and (η_5-C_5Me_4H) for complexes A1 and T1, respectively.

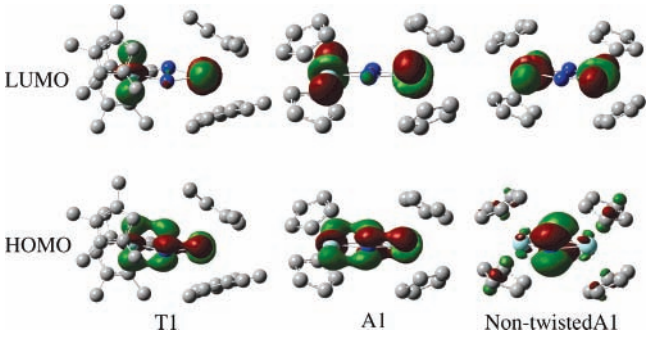

Figure 3. Frontier molecular orbitals (HOMO and LUMO) of complexes T1, A1, and nontwisted A1.

effectiveness of our modeling, we have calculated the energy of A1 as a function of the dihedral angles. The four ligands were twisted, and the dihedral angle was set to −52° for the global minimum optimized structure (see Figure 1, A1). This value was close to the value of −65° of T1 (Figure 1, T1). The difference in bond lengths was <0.02 Å for N−N and Zr−N, and it was 0.04 Å at the most for Zr−X. The $Zr-N_2-Zr$ structures were planar for both complexes.

Once we decided that complex A1 had a twisted structure, the electronic properties of complexes A1 and T1 were confirmed. Table 1 shows the Mulliken atomic charges of selected atoms and atom groups. All the values are in close agreement (with a difference of <0.05), and show the same trend. The electronic attraction and repulsion of both complexes and an approaching H_2 molecule are expected to be the same from these data, although there is a difference in steric effects. Figure 3 shows the frontier molecular orbitals of a twisted complex A1, a nontwisted complex A1, and complex T1. Pool et al.[17] proposed that the HOMO of complex T1 is suited for the coordination of N_2 side-on, and the LUMO is suited for H_2 addition, with which we also agree. Because complex A1 in Pool et al.'s calculations was confined to a nontwisted structure, the properties of the HOMO and LUMO were different from those of complex T1. Since we decided that complex A1 has a twisted form, we propose that the HOMO and LUMO of complexes A1 and T1 have the same properties, as shown in Figure 3. Therefore, from the results and discussion above, the effectiveness of the modeling has been ensured.

3.2. Addition of the First H_2 Molecule to Complex A1. The first step of the reaction is the coordination of H_2 that directly leads to the activation of the H−H bond producing the diazenidohydride complex $Cp_2Zr(\mu_2,\eta^2\text{-}N_2H)ZrCp_2(\mu\text{-}H)$, via a transition state, A2(TS). This can be described as a four-center transition state composed of an added H_2 and two centers, Zr^1 and N^1, where the H−H bond is broken at the same time as the Zr^1-H^2 and N^1-H^1 bonds are formed. Since the structure of the five C atoms of the Cp ring is stable, we focused on the local structure around the $Zr-N_2-Zr$ moiety (the identical four core atoms of the complexes), X, and the added H_2. There are some structural changes that should be noted in complexes A1−A3. The significant structural change in $Zr-N_2-Zr$ is that the

planar structure in complex A1 becomes nonplanar, since the H^1 atom pulls the N^1 atom into a bent structure, which is hinged at the N^1-N^2 axis in complex A3. The N^1-N^2 bond length elongates from 1.37 to 1.47 Å, which indicates a weakened N−N bond. It is reasonable that after the coordination of H_2 to Zr^1-N^1 that the bond length should increase by 0.10 Å. An increase in 0.09 and 0.06 Å for Zr^1-N^2 and Zr^2-N^1, respectively, and a decrease of 0.11 Å for Zr^2-N^2 are reasonable. The transitions of the dihedral angle, X−Zr−Zr−X, are shown in Figure 1 viewed along the Zr^2 to Zr^1 direction.

The barrier height of the addition of H_2 to complex A1 was calculated to be 20.4 kcal/mol. The product of the reaction, complex A3, was 12.1 kcal/mol exothermic relative to the reactants, complex A1 and H_2.

3.3. Migration of H^2 from the Zr Site to the N Site for Complex A3. Two reaction paths starting from complex A3 must be considered. One is the migration of H^2 from the Zr^1 site to the N^1 site. From complex A3, H^2 directly migrates from the Zr^1 site to the N^1 site while the N−N bond cleaves, and the changes in bond length of the Zr−N group take place at the same time through a transition state, A4(TS). The structure of the $Zr-N_2-Zr$ group becomes planar again in the product, complex A5, which is the analogue of complex T3. The more important change is the increase in the N−N bond distance, 1.47 Å in complex A3 to 2.78 Å in complex A5, indicating the complete cleavage of the N−N bond. The bond length increases for Zr^1-N^1 and Zr^2-N^1, and decreases for Zr^1-N^2 and Zr^2-N^2, reflecting the coordination complexity of the structure. The barrier height of this migration was calculated to be 34.7 kcal/mol, and the product was 57.9 kcal/mol exothermic relative to complex A3, as shown in Figure 2. We also considered the migration of H^2 to the other N^2 site, but since this type of migration requires H^2 to transfer across the Zr−Zr axis, where there must be a strong electronic repulsion, we concluded that this type of migration does not take place, or only seldom occurs compared to the migration producing complex A5.

3.4. Addition of the Second H_2 and the Ensuing Transformation of H. The other reaction from complex A3 is a second addition of H_2 taking place at the Zr^2 and N^2 sites, in contrast to the first H_2 addition at the Zr^1 and N^1 sites. The addition of H_2 results in the formation of H^3-N^2 and H^4-Zr^2 bonds via a transition state, A6(TS), which has a structure very similar to that of A2(TS), producing complex A7. The two N−H bonds in complex A7 are aligned in opposite directions, making the core region relatively symmetric, and this makes the $Zr-N_2-Zr$ group planar again. The barrier height of the addition of H_2 to complex A3 was calculated to be 10.9 kcal/mol, and the product of the reaction, A7, was 18.0 kcal/mol exothermic relative to the reactants, complex A3 and H_2.

The experimentally isolated structure, T2, had a bent $Zr-N_2-Zr$ structure, and the two N−H bonds are aligned in the same direction in our calculations, as shown in Figure 1. This means that complex A7 is not the analogue of complex T2. We considered the transformation that follows the second addition of an H_2 molecule. This transformation was calculated to take place via two transition states, and a reaction without a transition state. The barrier heights for the two transition states were calculated to be 13.8 and 2.0 kcal/mol, respectively. The product of the transformation series of complex A12, which is the analogue of complex T2, was 7.6 kcal/mol exothermic relative to complex A7 and 25.6 kcal/mol exothermic relative to complex A3 and H_2. The structure of complex A12 was in close agreement with that of the experimentally observed structure of complex T2, indicated in Figure 1.

3.5. Third and Fourth Additions of H_2 Starting from Complex A12. We performed calculations on the third and fourth additions of H_2 starting from complex A12. We eliminated the possibility of complex A7 being an initial complex for the ensuing H_2 addition, because of experimental reports that state complex T2 was the isolated structure.

The third addition of H_2 takes place at the Zr^2 and N^1 sites (here the two Zr and two N atoms are not distinguished), as in the previous additions forming Zr^2-H^6 and N^1-H^5 bonds via a transition state A13(TS), producing complex A14. The Zr^2-N^1 bond is elongated to 3.37 Å, which indicates a broken or very weak bond. This is because of the high coordination complexity around the Zr^2 and N^1 sites resulting in a destabilization of the $Zr-N_2-Zr$ structure. The barrier height was calculated to be 25.1 kcal/mol, and the product, complex A14, was 5.7 kcal/mol endothermic relative to complex A12 and H_2. Although this reaction is endothermic, the energy difference is so small that the reaction is expected to proceed under appropriate warming. Migration of the H^6 atom was considered in the same way as discussed in subsection 3.3, and was rejected. Since the N^1 atom already has two H atoms coordinated to it, inevitably the destination of an H^6 atom migration is the N^2 site, which we concluded to be energetically unfavorable in subsection 3.3.

Therefore, the initial complex of the fourth addition of H_2 must be complex A14, which reacts with H_2 in the same way as the third H_2 addition does. The H_2 addition takes place at the Zr^1 and N^2 sites to form Zr^1-H^8 and N^2-H^7 bonds via a transition state, A15(TS), producing a relatively symmetric complex, complex A16. The Zr^1-N^2 bond length is elongated to the same value as that of Zr^2-N^1. The Zr^1-N^1 and Zr^2-N^2 bond lengths were equal to each other. The barrier height was calculated to be 28.3 kcal/mol, and the product, complex A12, was 0.2 kcal/mol exothermic relative to complex A14 and H_2.

4. Discussion

4.1. Explanations (Correspondence and Accordance) of the Experimental Reactions of Complex T1 from Calculations Using Model Complex A. In this subsection, we give deep insight into the reaction mechanism and discuss correspondence between the experimentally required conditions of the experimental complex T1 and calculated results of our model complex.

Experimentally, the first and second additions of H_2 to T1 proceed immediately at room temperature. This can be understood from the energetics shown in Figure 2. The barrier height of the second H_2 addition is much lower than the barrier for the first H_2 addition. It is also worth mentioning that the second barrier is below the energy of complex A1 and $2H_2$. In other words, the activation energy is lower than the 12.1 kcal/mol stabilization of complex A3 relative to complex A1. This explains the reason for the immediate reaction of complex T1 with two H_2 molecules in series, forming not complex T3, but complex T2, as the product. One possible reason for the extremely low barrier height of the second H_2 addition compared to the first H_2 addition arises from the geometric changes that accompany the H_2 addition. The first H_2 addition is accompanied by an N−N bond stretch from 1.37 Å for complex A1 to 1.47 Å for complex A3. In contrast, complex A3 already has an elongated N−N bond, so that there is no need for an N−N stretch in the second H_2 addition, which should result in lower activation energy.

The transformation of H after the second H_2 addition was considered based on the experimental data mentioned in

subsection 3.4. This transformation of H was calculated to produce complex A12, the analogue of the experimentally isolated structure, complex T2, which was slightly more stable than complex A7. The barrier height of the transformation was lower than complex A3. This is a reasonable result, and it also suggests a reasonably free transformation of the atoms in the center of the complex. The reason for the stabilization of complex A12 relative to complex A7 can be explained by the stronger interaction of the Zr−Zr bond, since complex A12 has a bent Zr−N_2−Zr group, implying that there is a shorter Zr−Zr bond distance.

Another explanation is for the reaction of complex T2 after it is produced. Complex T2 may be the initial complex for further H_2 addition, or it could lose one H_2 molecule and transform into complex T3 through migration of H. The barrier height is 25.1 kcal/mol for the third addition of H_2, while it is 36.5 kcal/mol for the loss of H_2, which is the reverse reaction of the second H_2 addition, and it is 34.7 kcal/mol for H migration. The overall barrier height will be 60.3 kcal/mol for the latter process. This result tells us that, under conditions of excess H_2 and at moderate temperatures, the further addition of H_2 is likely to proceed. The requirement for gentle warming for further H_2 addition can be understood from the barrier heights gradually becoming higher as the reaction from complex A12 proceeds (25.1 and 28.3 kcal/mol for the third and fourth additions of H_2, respectively). It is also worth mentioning that the barrier height for the third addition of H_2 is relatively higher than that of the first and second additions. The third H_2 addition is the only H_2 addition that is a distinct endothermic reaction. In addition, the reverse reaction of the third H_2 addition is expected to occur since it is endothermic with 19.4 kcal/mol barrier height, which is lower than that of the fourth H_2 addition. Thus, these results match the experimental rate-controlling step and could be reasons for the low experimental yield of ammonia.

The negative vibration frequencies of the transition-state structures were −1390 and −1240 for the former two H_2 additions and −358 and −397 for the latter two H_2 additions, showing a recognizable difference between the two groups. The H−H bond lengths of approaching H_2 molecules also show the same difference between the two groups (Figure 1). Thus, it is expected that the difference in the barrier heights and reaction rates of the former two and latter two H_2 additions can be explained in terms of the structural changes and electronic states. For the former two H_2 additions, only the approaching H atoms show movement through the transition state. This mechanism is similar to the mechanism presented in the publication by Basch et al.[13] In contrast, for the latter two H_2 additions, the Zr and N atoms in the center move as well as the approaching H atoms. This results in a higher barrier and unstable products. We will discuss this further using the electronic states of the complexes in a future publication.

On the other hand, at high temperatures, such as in the experimental boiling heptane solution, the formation of complex T3 is advantageous. Once the energy is adequate for the formation of complex T3, then it is expected that this process will proceed, since the reaction is 57.9 kcal/mol exothermic, which is a large stabilization energy. Experimentally, ammonia produced by further addition of H_2 to complex T2 is found in low yield. This can be explained by comparing the barrier heights for the two reactions that T2 follows, as explained above. The difference between the third H_2 addition and the loss of H_2 is only 11.4 kcal/mol under heating conditions, so both reactions are expected to occur. This could also be a reason for the low experimental yield of ammonia in addition to the reverse reaction of third H_2 addition discussed in the previous paragraphs.

4.2. Correspondence and Distinction between the Reactivity of Complexes A1 and P1. Comparing the results of our study and Bacsh et al.'s study,[13] we can derive significant information and indications about hydrogenations of N_2 with side-on Zr−N−N−Zr complexes. Since the exchange-correlation functional and basis sets adopted in the DFT calculation in ref 13 were different from those in our calculations for complex A, we have recalculated the model complex of P1 and its derivatives. We were able to calculate optimized structures that closely resemble the structures shown in ref 13 in the level of our calculation. From here, the derivatives of P1 corresponding to that of complex A will be denoted with an prime (e.g., complex A′, A1′ denotes model complex of P1).

We focused on the reaction path that corresponds to the reaction path of complex A. For the first H_2 addition, the reaction mechanism is similar as mentioned in the previous section. The barrier heights of the reactions with A1 and A1′ show little difference (20.4 and 23.7 kcal/mol, respectively) and are both sufficiently endothermic. We could easily imagine from the prediction in ref 13 that A1 can undergo the same H_2 addition.

The difference appears for the second H_2 addition. The reaction mechanism is similar again for complex A and path II in ref 13 which starts from A3 and A3′, respectively. However, the barrier heights are 10.9 and 24.0 kcal/mol for complex A and complex A′, respectively, which differ significantly. We should mention that, in contrast to complex A, the barrier height of complex A′ for second H_2 addition is higher than that for the first H_2 addition and it is above the energy of complex A1′ and $2H_2$. The stabilization through the reaction is also different as shown in Figure 4.

There was another reaction path mentioned in ref 13 (path I) for complex A′ with the second H_2 addition. The reaction starts from an isomer of A3′, which has a bridging H atom between the Zr atoms, forming after the first H_2 addition. This reaction has a slightly smaller barrier height than that of path II. However, the reaction starting from the isomer is endothermic and it is more likely to proceed to the reverse direction since the reactions following have higher barrier heights. We also considered the corresponding structure of the isomer for complex A. However, starting from many structures, we were not able to calculate a corresponding structure since they converted into A5 or an isomer of A5. The bending of Zr−N_2−Zr structure is smaller in A3 than A3′, resulting in longer lengths between the two Zr atoms and bridging H atom in A3 relative to A3′.

Therefore, we have presented in terms of energetics that complex A′, which is a model of the experimental complex P1 and its derivatives, is not reactive as much as complex A for the second H_2 addition. From the discussion in the previous section and here, it is clearly shown that complex A is expected to react immediately with two H_2 molecules while complex A′ only reacts with one H_2 molecule. It is interesting that the difference in the ligands shows this significant distinction. We are now studying the reasons for the energetics in terms of structures and electronic states which will be presented soon.

More definitive differences between the present model complexes and the Basch et al.'s model complexes may appear in the reactions following. Basch et al.'s model complexes require constraints on the distance between Zr and P atoms that give unphysical structures. However, with no constraints on the distance, no stable structures are found. Thus, it is possible that the undergoing reactions are different from those of Fryzuk et

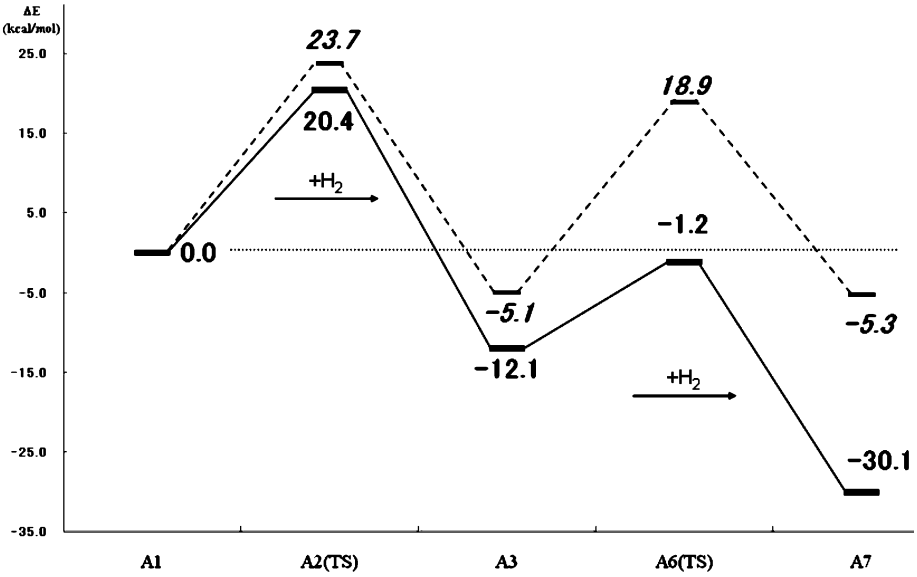

Figure 4. Calculated reaction potential energy diagram of the reactions with two H_2 molecules for complex A and model complex of P1, which was proposed by Basch et al. as explained in the Introduction. The numbers in italics are the energies of complex A′, which are P1 and its derivatives corresponding to complex A.

al.'s experiments. In our calculations, no restriction on the optimization is imposed. The present study shows that the distance from the Zr atoms to the X (where X is the weighted center of the five C atoms of Cp) changes a little, while the dihedral angle of X−Zr−Zr−X changes drastically during the hydrogen additions. The latter indicates that mechanically flexible ligands are favorable in the series of the hydrogen additions. In fact, Fryzuk et al.'s system has large and stiff ligands, and second or more hydrogen addition reactions do not occur in his system while they did in the calculations with Basch et al.'s model complexes. We could consider that the model ligands of Basch et al.'s model complexes were more flexible, which is suitable for the hydrogen additions, than the real ligands in the experiment since the only constrained parameter is the bond lengths, meaning that the angles or the dihedrals are free. The importance of the mechanical flexibility of the ligands will be presented in detail elsewhere.

4.3. Reactions of Complex A16. The final step of this series of reactions is the production of NH_3 and complex A17 from complex A16. There are many possibilities for this type of bond-breaking processes, and it is difficult to deal with all of them using quantum chemical calculations. We may have to adopt some other methods, such as molecular dynamics calculations, to find the exact transition state and reaction path. Since the main subject of this paper is a study of H_2 addition and its relationship to experimental data, we will impose a restriction on the breaking processes by considering several bond lengths to be the same as those of the reactants. Under this restriction, we will only refer to the energies of the equilibrium structures. Although we were not able to calculate the energetics to the same accuracy as in the above results, the estimations of the energetics are reasonably accurate.

We considered two reactions that complex A16, $(\mu\text{-H})_2Cp_2\text{-}Zr(\mu_2,\eta^2\text{-}N_2H_4)ZrCp_2(\mu\text{-H})_2$, may follow. The first reaction is the addition of a fifth H_2 molecule, forming two mononuclear Zr complexes, A17, and two equivalents of NH_3, for which we were not able to calculate the transition state. We speculated that the barrier height from another H_2 addition may be some 30 kcal/mol, although it might be higher. The products were calculated to be 1.2 kcal/mol exothermic relative to complex A16.

The second reaction is the cleavage of complex A16 into two mononuclear Zr complexes and N_2H_4, which may be followed by reduction of the hydrazine to ammonia. We conducted calculations to obtain the potential energy curve in terms of the Zr−N bond distance. This indicated the barrier height to be approximately 50 kcal/mol. The two Zr complexes and hydrazine were 39.0 kcal/mol endothermic relative to complex A16. It is known that molecules of hydrazine can react to produce ammonia. Though the barrier is relatively high, the second reaction followed by a reaction of the hydrazine may be more likely. Since the Zr atom of complex A16 appears to be associated with H atoms, we supposed that the four-center transition state, which requires an interaction of Zr and H, will not occur for the fifth H_2 addition. This is the subject of present calculations and analysis and will be reported in another publication soon.

4.4. Treatment of the Effect of the Solvent. We note that our calculations presented in the Results section were calculated in the gas phase, and that no solvent effects were taken into account. Although these reactions are homogeneous, and it is better to include solvent effects, we could only include these effects on a model, as the use of a solvent model requires extremely high computer resources. The small dipole moment of the calculated structures indicates that the effect of organic solvents used in experiments must be small.

We have confirmed our presumption to support our discussion by calculating the single point energies of complex A. The calculations were carried out using the PCM method[28−31] implemented in the Gaussian 03 software package.[22] Heptane was used as the solvent for all the complexes, since it was most convenient to use. The energies of each structure were different by 1.5 kcal/mol on average, and 5.4 kcal/mol at the most, with the A15(TS) complex lowering the barrier from 28.0 to 24.7 kcal/mol. These differences are small enough, and we concluded that calculations in the gas phase are sufficiently accurate to reliably determine the nature of the reactions.

5. Conclusions

We have theoretically studied the structures, energetics, and reaction mechanisms of several H_2 additions and H migrations

in a series based on a model complex, $(Cp_2Zr)_2(\mu_2,\eta^2,\eta^2\text{-}N_2H_2)$ (A1). First, the effectiveness of our model complex for the experimental complex was considered in terms of the structures, energetics, the Mulliken atomic charges, and the frontier molecular orbitals. From the structures obtained, we suggest that the structure of complex A1 is twisted, and resembles the structure of the initial experimental complex, $[(C_5Me_4H)Zr]_2(\mu_2,\eta^2,\eta^2\text{-}N_2H_2)$ (T1). The electronic properties of the twisted complex A1 were in close agreement with those of the experimental complex T1. Hence, complex A1 was expected to follow the same reaction path as the experimental complex T1. Therefore, we decided that it is effective to adopt complex A to study the reactions of the experimental complex. Furthermore, the calculated structures and energies of complexes T2, T3, and T4 (derivatives from T1 and H_2 addition) were in close agreement with the calculations of complex A, supporting the effectiveness of our modeling.

With our reasonable model complex, we have theoretically presented the full reaction path of complex A1 for four H_2 additions, and we suggest two reaction paths that can occur to account for the experimental dinitrogen fixation process with complex T1 and several H_2 molecules. From our results, we have derived the following interesting conclusions: Reactions of complex A1 with H_2 proceed in a series via a four-center transition state that includes an added H_2 and two Zr and N centers. The energetics, such as the energy barriers and structural changes for each H_2 addition, can explain the experimental results and required conditions clearly.

In experiments, the addition of two H_2 molecules proceeds immediately, producing $[(\eta_5\text{-}C_5Me_4H)_2ZrH]_2(\mu_2,\eta^2,\eta^2\text{-}N_2H_2)$ (T2). There are two reaction paths that complex T2 can follow. One is the addition of a third or more H_2 molecules, and the other is to lose one H_2 molecule and a migration of H. The former reaction path proceeds under gentle warming, while the latter reaction path proceeds in boiling heptane at temperatures near 100 °C. The calculated four energy barriers for H_2 addition were 20.4, 10.9, 24.1, and 28.0 kcal/mol, respectively, and the energy barrier for H migration was 60.3 kcal/mol overall. The barrier for the second H_2 addition is much lower than those for the other H_2 additions, and was below the energy for complex A1 and $2H_2$, indicating that it is an immediate process. This low energy barrier can be explained from structural changes occurring during H_2 additions.

The two reactions of complex T2 that are dependent on the experimental conditions can be explained by comparing the energy barriers and stabilization energies for the third H_2 addition and H migration. Since the energy barrier is lower for the third H_2 addition, this reaction path is expected to be taken at low temperatures. On the other hand, because H migration is largely exothermic, at high temperatures, this path is more likely to be taken. Furthermore, general heating, which is an experimental condition for the third and further H_2 additions to occur, is required, since the energy barrier gradually increases as the reaction proceeds. The higher barrier of the third H_2 addition compared to the first and second H_2 additions, the result that the third H_2 addition is the only distinct endothermic reaction, the low barrier for the reverse reaction of the third H_2 addition, and the side reaction from T2 to T3 account for the low experimental yield of ammonia.

The correspondence and distinction between the reactivity of complex A and that of complex A′, which is a model complex of $[P_2N_2]Zr(\mu_2,\eta^2,\eta^2\text{-}N_2)Zr[P_2N_2]$ (P1) and its derivatives previously studied by Basch et al., has also been presented since the reactions of both complexes are similar. We have presented that the higher reactivity of complex A relative to complex A′ could be explained in terms of the calculated energetics. The barrier for the second H_2 addition to complex A′ (24.0 kcal/mol) was as high as the first H_2 addition (23.7 kcal/mol) in contrast to complex A mentioned above. We have also stated the importance of the flexibility of ligands coordinated to Zr atoms. This arises from the fact that Zr−X (the weighted center of the five C atoms of Cp) distances change little while the dihedral angles X−Zr−Zr−X change drastically. The latter indicates that mechanically flexible ligands are favorable in the series of the hydrogen additions. The comparison of the stiffness of the ligands in the experimental complex P1 and model complex A′ also indicates this idea.

There is still much work to be done, which we are planning to present soon. One of these tasks is to compare the calculations on the model complex A with data from an experimental complex, or from other complexes with different ligands. The experimental complex T1 and other complexes with different ligands such as P1 are being investigated in calculations. We expect that the results of those calculations along with the results presented in this paper will help clarify the mechanism of nitrogen reduction using binuclear metal complexes. We greatly welcome contact with experimentalists to discuss this.

Acknowledgment. This research was supported in part by a Grant-in-Aid for Specially Promoted Research "Simulations and Dynamics for Real Systems", and the Grant for 21st Century COE Research "Human-Friendly Materials based on Chemistry" from the Ministry of Education, Science and Culture, and Sports of Japan.

Supporting Information Available: Geometry, in Cartesian coordinates, and total energies of all structures presented in this paper. This material is available free of charge via the Internet at http://pubs.acs.org.

References and Notes

(1) Fryzuk, M. D.; Johnson, S. A. *Coord. Chem. Rev.* **2000**, *200*, 379.
(2) Shaver, M. P.; Fryzuk, M. D. *Adv. Synth. Catal.* **2003**, *345*, 1061.
(3) Schlögl, R. *Angew. Chem., Int. Ed.* **2003**, *42*, 2004.
(4) Fryzuk, M. D.*Chem. Rec.* **2003**, *3*, 2.
(5) Nishibayashi, Y.; Iwai, S.; Hidai, M. *Science* **1998**, *279*, 540.
(6) Yandulov, D. V.; Shrock, R. R. *Science* **2003**, *301*, 76.
(7) Fryzuk, M. D.; Love, J. B.; Rettig, S. J.; Young, V. G. *Science* **1997**, *275*, 1445.
(8) Pool, J. A.; Lobkovsky, E.; Chirik, P. J. *Nature* **2004**, *427*, 527.
(9) Fryzuk, M. D. *Nature* **2004**, *427*, 498.
(10) Blomberg, M. R. A.; Siegbahn, P. E. M. *J. Am. Chem. Soc.* **1993**, *115*, 6908.
(11) Basch, H.; Musaev, D. G.; Morokuma, K. Fryzuk, M. D.; Love, J. B.; Seidel, W. W.; Albinati, A.; Koetzle, T. F.; Klooster, W. T.; Mason, S. A.; Eckert, J. *J. Am. Chem. Soc.* **1999**, *121*, 523.
(12) Basch, H.; Musaev, D. G.; Morokuma, K. *J. Am. Chem. Soc.* **1999**, *121*, 5754.
(13) Basch, H.; Musaev, D. G.; Morokuma, K. *Organometallics* **2000**, *19*, 3393.
(14) Honkala, K.; Hellman, A.; Remediakis, I. N.; Logadottir, A.; Carlsson, A.; Dahl, S.; Cristense, C. H.; Nørskov, J. K. *Science* **2005**, *307*, 555.
(15) Fryzuk, M. D.; Haddad, T. S.; Mylvaganam, M.; McConville, D. H.; Rettig, S. J. *J. Am. Chem. Soc.* **1993**, *115*, 2781.
(16) Musaev, D. G. *J. Phys. Chem. B* **2004**, *108*, 10012.
(17) Pool, J. A.; Bernskoetter, W. H.; Chirik, P. J. *J. Am. Chem. Soc.* **2004**, *126*, 14326.
(18) Becke, A. D. *Phys. Rev. A* **1988**, *38*, 3098.
(19) Becke, A. D. *J. Chem. Phys.* **1993**, *98*, 5648.
(20) Lee, C.; Yang, W.; Parr, R. G. *Phys. Rev. B* **1988**, *37*, 785.
(21) Miehlich, B.; Savin, A.; Stoll, H.; Preuss, H. *Chem. Phys. Lett.* **1989**, *157*, 200.
(22) Frisch, M. J.; Trucks, G. W.; Schlegel, H. B.; Scuseria, G. E.; Robb, M. A.; Cheeseman, J. R.; Montgomery, J. A., Jr.; Vreven, T.; Kudin, K. N.; Burant, J. C.; Millam, J. M.; Iyengar, S. S.; Tomasi, J.; Barone, V.;

Mennucci, B.; Cossi, M.; Scalmani, G.; Rega, N.; Petersson, G. A.; Nakatsuji, H.; Hada, M.; Ehara, M.; Toyota, K.; Fukuda, R.; Hasegawa, J.; Ishida, M.; Nakajima, T.; Honda, Y.; Kitao, O.; Nakai, H.; Klene, M.; Li, X.; Knox, J. E.; Hratchian, H. P.; Cross, J. B.; Bakken, V.; Adamo, C.; Jaramillo, J.; Gomperts, R.; Stratmann, R. E.; Yazyev, O.; Austin, A. J.; Cammi, R.; Pomelli, C.; Ochterski, J. W.; Ayala, P. Y.; Morokuma, K.; Voth, G. A.; Salvador, P.; Dannenberg, J. J.; Zakrzewski, V. G.; Dapprich, S.; Daniels, A. D.; Strain, M. C.; Farkas, O.; Malick, D. K.; Rabuck, A. D.; Raghavachari, K.; Foresman, J. B.; Ortiz, J. V.; Cui, Q.; Baboul, A. G.; Clifford, S.; Cioslowski, J.; Stefanov, B. B.; Liu, G.; Liashenko, A.; Piskorz, P.; Komaromi, I.; Martin, R. L.; Fox, D. J.; Keith, T.; Al-Laham, M. A.; Peng, C. Y.; Nanayakkara, A.; Challacombe, M.; Gill, P. M. W.; Johnson, B.; Chen, W.; Wong, M. W.; Gonzalez, C.; Pople, J. A. *Gaussian 03*; Gaussian, Inc.: Wallingford, CT, 2004.

(23) Hay, P. J.; Wadt, W. R. *J. Chem. Phys.* **1995**, *82*, 270.

(24) Wadt, W. R.; Hay, P. J. *J. Chem. Phys.* **1985**, *82*, 284.

(25) Hay, P. J.; Wadt, W. R. *J. Chem. Phys.* **1985**, *82*, 299.

(26) Gonzalez, C.; Schlegel, H. B. *J. Chem. Phys.* **1989**, *90*, 2154.

(27) Gonzalez, C.; Schlegel, H. B. *J. Phys. Chem.* **1990**, *94*, 5523.

(28) Cancès, M. T.; Mennucci, B.; Tomasi, J. *J. Chem. Phys.* **1997**, *107*, 3032.

(29) Cossi, M.; Barone, V.; Mennucci, B.; Tomasi, J. *Chem. Phys. Lett.* **1998**, *286*, 253.

(30) Mennucci, B.; Tomasi, J. *J. Chem. Phys.* **1997**, *106*, 5151.

(31) Cossi, M.; Scalmani, G.; Rega, N.; Barone, V. *J. Chem. Phys.* **2002**, *117*, 43.